Protein Dimerization

Deutsche Ausgabe: DOI: 10.1002/ange.201506686
Internationale Ausgabe: DOI: 10.1002/anie.201506686

Rational Structure-Based Design of Bright GFP-Based Complexes with Tunable Dimerization

*Majid Eshaghi, Guangyu Sun, Andreas Grüter, Chiew Ling Lim, Yuemin Celina Chee, Gregor Jung, Ralf Jauch, Thorsten Wohland, and Swaine L. Chen**

Abstract: *Fluorescent proteins are transformative tools; thus, any brightness increase is a welcome improvement. We invented the "vGFP strategy" based on structural analysis of GFP bound to a single-domain antibody, predicting tunable dimerization, enhanced brightness (ca. 50%), and improved pH resistance. We verified all of these predictions using biochemistry, crystallography, and single-molecule studies. We applied the vsfGFP proteins in three diverse scenarios: single-step immunofluorescence in vitro (3× brighter due to dimerization); expression in bacteria and human cells in vivo (1.5× brighter); and protein fusions showing better pH resistance in human cells in vivo. The vGFP strategy thus allows upgrading of existing applications, is applicable to other fluorescent proteins, and suggests a method for tuning dimerization of arbitrary proteins and optimizing protein properties in general.*

The key biochemical feature of GFP that enables most applications is its ability to spontaneously fold as a single domain, resulting in a nontoxic, stable fusion partner.[1–5] In particular, fusion to antibodies enables a large array of additional in vivo and in vitro applications.[3,6,7] Recently, single-domain antibodies, or nanobodies, that bind to GFP (green fluorescent protein) and modulate its fluorescence have resulted in additional tools.[8–13] One of these nanobodies, the Enhancer (not to be confused with the "enhanced" in EGFP), results in a 50% increase in EGFP fluorescence upon binding, enabling new applications where the Enhancer and EGFP are fused to separate proteins.[8,14] We here describe a twist on the use of the Enhancer nanobody, termed the "vGFP strategy", enabling increased brightness in more common applications of GFP such as fusion proteins or as a cell marker. The vGFP design further enables rational control of dimerization, leading to improved signal in diverse in vitro and in vivo applications. A similar strategy could provide similar benefits to other fluorescent proteins.

The crystal structure of the Enhancer nanobody bound to GFP[11] shows that the C-terminus of the GFP β-barrel emerges at a radial location overlapping the Enhancer binding site but from the opposite "lid". The Enhancer N-terminus lies on the most proximal surface of the Enhancer to the GFP C-terminus, at a distance of 29.5 Å (Figure 1a). We predicted that joining these termini with 9 amino acids (assuming a 3.5 Å axial Cα–Cα distance for extended β-strands)[15] would allow formation of the native complex by reflexive intramolecular binding. Coincidentally, GFP has 9 unstructured amino acids at its C-terminus, which can therefore connect the structured part of the GFP β-barrel to the Enhancer (we refer to this as vGFP-9, Figure 1b, top). In contrast, direct fusion of the Enhancer to the structured C-terminus of the GFP β-barrel (i.e. truncating the unstructured 9aa) would preclude reflexive binding and thereby form a dimer (vGFP-0, Figure 1b, bottom). Based on entropic considerations, we expected that vGFP-9, while capable of forming a dimer, would favor monomerization, thus forming a stably folding protein with the improved brightness of an enhanced GFP, enabling use as a drop-in replacement for GFP. vGFP-0, in contrast, would theoretically have a single particle brightness of twice that of vGFP-9, providing an advantage when dimerization can be tolerated.

vsfGFP constructs [using superfolder GFP (sfGFP)[16] as the base GFP] were fluorescent in both the cytoplasm and periplasm of *E. coli* (Figure 1c and Figure S1a in the Supporting Information). Purified proteins formed the expected monomer (vsfGFP-9) and dimer (vsfGFP-0) by chromatography and light scattering (Figure S1b and S1C), with negligible aggregation. Finally, we saw the expected monotonic increase in monomer:dimer ratio as linker length increased from 0 to 9aa (Figure 1d). We therefore focused the rest of our studies on vsfGFP-0 and vsfGFP-9.

We determined the crystal structure of vsfGFP-0 to a resolution of 2.60 Å (statistics in Table S1). The asymmetric unit contained two vsfGFP-0 proteins with non-crystallographic 2-fold symmetry. The junction between domains was clearly visible, verifying that a dimer between two vsfGFP-0 molecules was formed (Figure 2a, arrowheads). The Enhancer:sfGFP complex in vsfGFP-0 (each domain from a differ-

[*] M. Eshaghi, C. L. Lim, Y. C. Chee, S. L. Chen
National University of Singapore, Department of Medicine, Yong Loo Lin School of Medicine, 1E Kent Ridge Road, NUHS Tower Block, Level 10, Singapore 119074 (Singapore)
G. Sun, T. Wohland
National University of Singapore, Departments of Chemistry and Biological Sciences and Center for Bio-Imaging Sciences Singapore 117557 (Singapore)
A. Grüter, G. Jung
Saarland University, 66123 Saarbrücken (Germany)
R. Jauch
Guangzhou Institutes of Biomedicine and Health, Chinese Academy of Sciences, Guangzhou 510530 (China)
S. L. Chen
Genome Institute of Singapore, Infectious Diseases Group
60 Biopolis Street, Genome, #02-01, Singapore 138672 (Singapore)
E-mail: slchen@gis.a-star.edu.sg

Supporting information (strains, plasmids, experimental procedures, and analyses) and ORCID(s) from the author(s) for this article are available on the WWW under http://dx.doi.org/10.1002/anie.201506686.

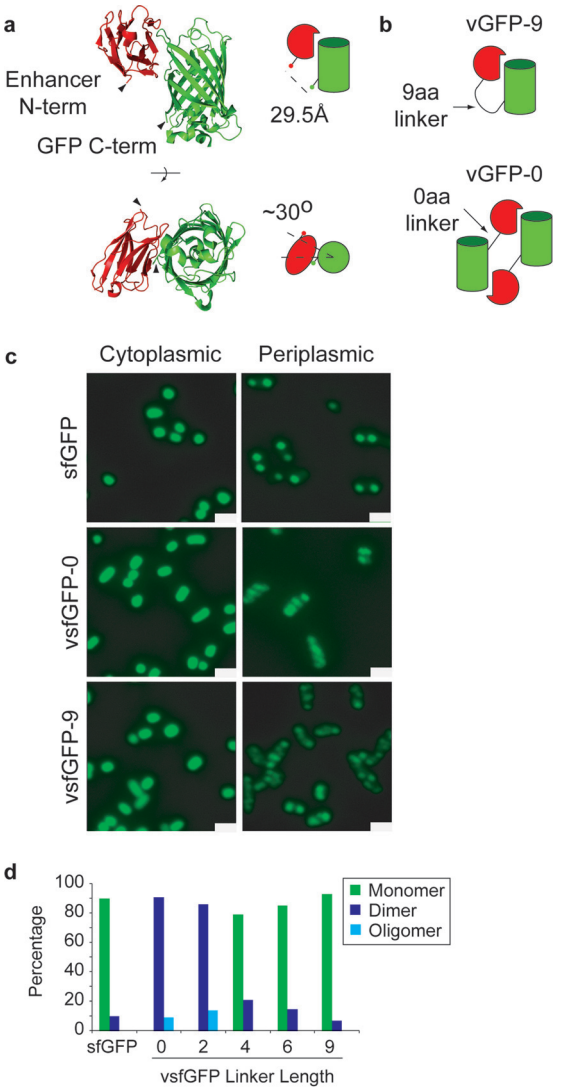

Figure 1. The vGFP strategy for tunable dimerization. a) Crystal structure from PDB 3K1K (left) and schematic (right) of GFP (green) bound to Enhancer (red). The GFP C-terminus and the Enhancer N-terminus are indicated by arrowheads on the left and colored dots on the right. The distance between these termini is indicated. (bottom) As above but rotated by 90° about the horizontal axis. The angle between the termini is indicated. b) Schematic of dimerization control in the vGFP fusion. Top: A 9aa linker in vGFP-9 enables reflexive binding of the Enhancer domain to the fused GFP domain. Bottom: A 0aa linker in vGFP-0 precludes reflexive binding, forcing formation of a dimer. c) Fluorescence micrographs (scale bar, 2 μm) of *E. coli* expressing cytoplasmic (left) and periplasmic (right) sfGFP, vsfGFP-0, and vsfGFP-9. d) Percentage of monomer (green), dimer (blue), and oligomers (cyan) for vsfGFP with linkers of varying length (indicated on *X*-axis).

ent protein) was similar to that of the reported the Enhancer:GFP complex[11] overall (Figure 2b) and based on side chain conformations at the Enhancer:sfGFP interface (Figure 2c and Figure S2a, RMSD = 0.86 Å over all atoms displayed) and surrounding the chromophore (Figure S2b, RMSD = 0.40 Å). Notably, His-148 of sfGFP was closer to the acidic proton of Tyr-66 in vsfGFP-0 than in the unbound GFP structure, suggesting that stabilization of the phenolate anion state of the chromophore (as previously noted[11]) would occur in the vsfGFP constructs as well, increasing fluorescence. We further predicted that vsfGFP constructs would have better robustness to acidic pH.

To test for increased brightness, we first verified that vsfGFP-0 and vsfGFP-9 had similar excitation and emission spectra to the parental sfGFP (Figure S3). Bulk fluorescence of purified proteins yielded relative molar brightnesses of 1.51× (vsfGFP-0) and 1.58× (vsfGFP-9) relative to sfGFP. Bulk purified protein, however, may contain misfolded or otherwise non-fluorescent proteins. We therefore measured single particle brightness using fluorescence correlation spectroscopy (FCS). vsfGFP-9 demonstrated 1.57× brightness compared with sfGFP, with a similar diffusion coefficient (Table 1, Table S2), verifying that fluorescent molecules of

Table 1: Fluorescence parameters for fluorescent proteins studied.

Protein	Calcd MW [Da]	pK_a	Quantum yield (QY)	ε_{488}[a] (relative to sfGFP)	Brightness (relative to sfGFP)[b]
EGFP	27800	5.67 ± 0.07	0.63 ± 0.06	0.67[25]	0.79 ± 0.02
sfGFP	27604	5.74 ± 0.05	0.68 ± 0.06	1	1
vsfGFP-0	39210.9	4.84 ± 0.13	0.76 ± 0.07	2.52 ± 0.40	2.93 ± 0.85
vsfGFP-9	40286.1	4.75 ± 0.12	0.70 ± 0.06	1.26 ± 0.19	1.57 ± 0.39

[a] ε_{488} (extinction coefficient at 488 nm) relative to sfGFP was taken from published values (for EGFP) or calculated by Ward's method[24] in three separate experiments (for vsfGFP-0 and vsfGFP-9; average (± SD) is shown). [b] Relative brightness values are the average (± SD) from 3 separate FCS experiments for EGFP and 4 experiments for vsfGFP-0 and vsfGFP-9

vsfGFP-9 are indeed monomeric and arguing that vsfGFP-9, despite its extra nanobody domain, has no size disadvantage compared with sfGFP. vsfGFP-0 showed 2.93× brightness compared to sfGFP, with a diffusion coefficient ~30% lower, consistent with a dimer having twice the single-particle brightness of vsfGFP-9. Furthermore, the vsfGFP constructs were comparable to sfGFP in quantum yield, higher in extinction coefficient (Table 1), similar in fluorescence lifetime (Table S3), and slightly improved in photostability (Table S4); therefore, the vsfGFP proteins compare favorably with other green FPs (Table S5). Finally, using FCS, we validated the prediction that the vsfGFP constructs would retain fluorescence better than sfGFP at low pH (3% residual fluorescence at pH 3.5 for sfGFP, 21% for vsfGFP-9, and 23% for vsfGFP-0 at 20 μW; Figure 3a). This pH robustness was supported by modeling demonstrating a pH-dependent dark state[17] affecting a larger fraction of sfGFP than vsfGFP-9 and vsfGFP-0 particles at low pH (Figure 3b, Table S6), while a photon-induced dark state[18] was similar among all proteins (Figure 3b and S4, Table S2). Bulk pK_a measurements also showed that vsfGFP-9 and vsfGFP-0 had pK_a values ca. 1 pH unit lower than sfGFP (Figure S5, Table 1). We thus validated all of the structure-based predictions regarding dimerization, brightness, and pH stability for the vsfGFP proteins.

We performed several practical applications to highlight the utility of the vsfGFP proteins. Effective fluorescence can depend on the environment in which it is measured; there-

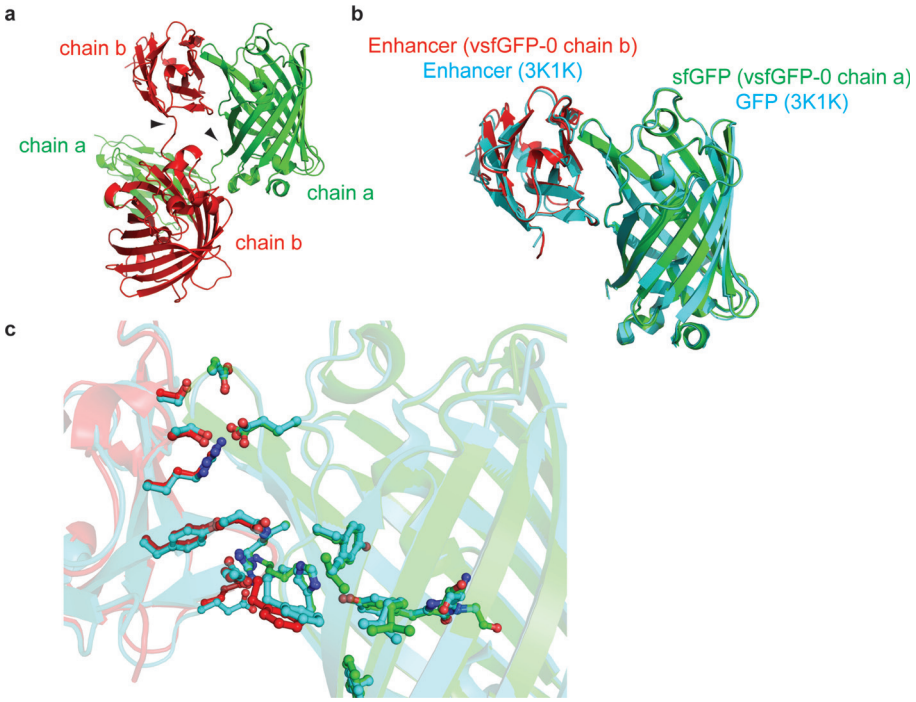

Figure 2. Crystal structure of vsfGFP-0. a) Cartoon representation of the unit cell of the vsfGFP-0 crystal structure. The GFP and Enhancer domains of one monomer (chain a) are green and of the other monomer (chain b) are red. Arrowheads indicate linkers between sfGFP and Enhancer domains. b) Superposition of the Enhancer:GFP complex in vsfGFP-0 (green, sfGFP; red, Enhancer) (this study) and PDB 3K1K (cyan for both proteins). c) Positions of amino acids at the interface of the GFP:Enhancer complex of PDB 3K1K (cyan) and of the vsfGFP-0 complex (red, Enhancer; green, sfGFP; domains are from different proteins). A cartoon representation of the GFP:Enhancer complex is shown in transparent cyan and of the vsfGFP-0 complex in transparent red (Enhancer domain) and green (sfGFP domain). For amino acid labels, see Figure S2.

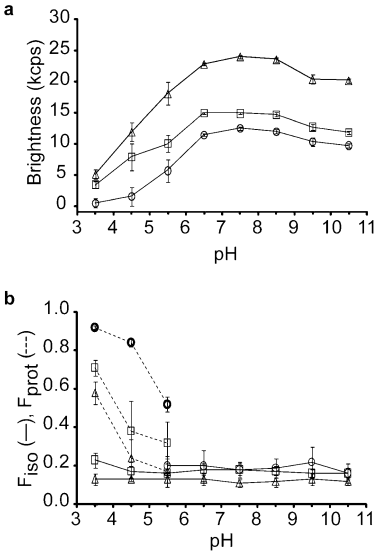

Figure 3. FCS measurements of vsfGFP variants. a) Single particle brightness as a function of pH at 20 μW laser power. b) Fraction of dark states from a model using one (F_{iso}, pH > 5.5) or two (F_{iso} and F_{prot}, pH < = 5.5) dark states. Error bars denote standard deviation. sfGFP (○), vsfGFP-0 (△), and vsfGFP-9 (□).

fore, we assayed brightness in living cells to ensure they still outperformed sfGFP. *E. coli* expressing vsfGFP-0 and vsfGFP-9 were 1.3× and 1.2× as bright, respectively, as those expressing sfGFP after correcting for expression levels, with no visible degradation, verifying that fluorescence was due to full-length proteins (Figure 4 and S6a,b). Given the uncertainty in quantifying protein levels in vivo, this increased brightness agrees well with our bulk and single molecule data. In human 293T cells, vsfGFP-0 seemed to form foci, but sfGFP and vsfGFP-9 were evenly distributed throughout the cytoplasm (Figure S6c). Both vsfGFP-0 and vsfGFP-9 were again inherently brighter than sfGFP (1.7× and 1.5×, respectively) after normalizing for protein levels (Figure S6d–g). vsfGFP-9 also bleached slightly more slowly than sfGFP in human cells under high- and low-intensity illumination (Figure S7), consistent with the better photostability measured by FCS. Finally, use of vsfGFP-9 in combination with optimized expression enabled more sensitive detection of a pathogenic strain of *E. coli* in in vivo assays without altering the course of infection.[19]

In a second application, we used vsfGFP constructs as labels for immunofluorescence. We fused an anti-cytokeratin-8 (CK8) nanobody[20] to the N-terminus of sfGFP, vsfGFP-0, and vsfGFP-9 and used these to staining of fixed HeLa cells. Co-staining with a conventional anti-CK8 monoclonal antibody confirmed proper staining of cytokeratin filaments (Figure 5a). vsfGFP-9 provided 2.0× the signal of the sfGFP fusion, while the vsfGFP-0 fusion resulted in a 3.4× increase (Figure 5b and Figure S8), demonstrating the advantage of dimerization.

As a final application, we tested the vsfGFP proteins as fusion partners. We fused mCherry to the N-terminus and LC3 (microtubule-associated protein 1 light chain 3)[21] to the C-terminus of sfGFP and vsfGFP-9. LC3 targets to autophagosomes that fuse with lysosomes, thus lowering pH and resulting in protein degradation; the mCherry (not pH sensitive) allows quantification of non-degraded protein,[22] enabling us to test the pH robustness of vsfGFP-9 in vivo. sfGFP and vsfGFP-9 fusions were of comparable stability, validating vsfGFP-9 as a drop-in replacement for sfGFP (Figure S9). As expected, the vsfGFP-9 fusion had brighter green fluorescence than sfGFP throughout the experiment (Figure 6a,b). At 6 h, lysosomal pH is approximately 5.5;[23] based on FCS, vsfGFP-9 should therefore provide a further 1.5× brightness increase over sfGFP when pH drops from 7.5

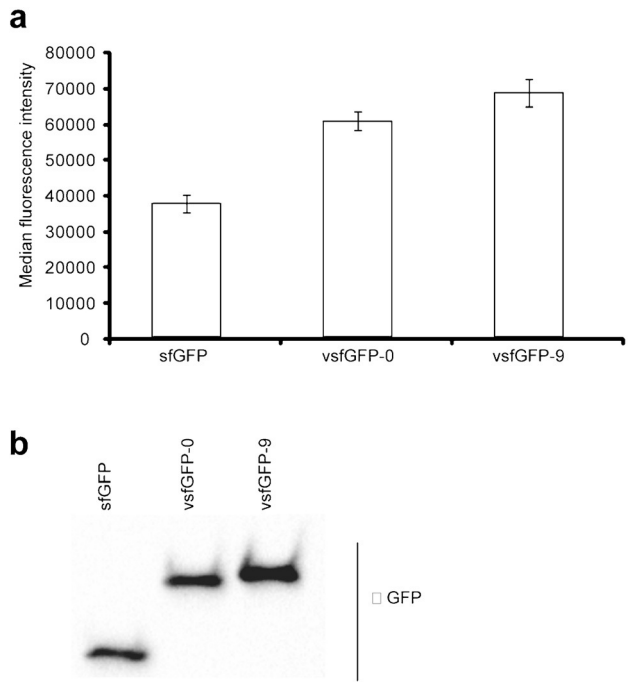

Figure 4. In vivo brightness of vsfGFP variants. a) Median fluorescence intensity of *E. coli* expressing sfGFP, vsfGFP-0, and vsfGFP-9 proteins measured by flow cytometry analysis. Error bars show standard deviations of three independent repeats. Normalized to sfGFP, vsfGFP-0, and vsfGFP-9 are 1.6× and 1.8× as bright, respectively. b) Quantification of GFP protein levels in *E. coli*. Immunoblot of samples from panel (a) using α-GFP antibody. By densitometry analysis, protein levels for vsfGFP-0 and vsfGFP-9 are 1.2× and 1.5× that of sfGFP, resulting in normalized inherent brightnesses of 1.3× and 1.2×, respectively.

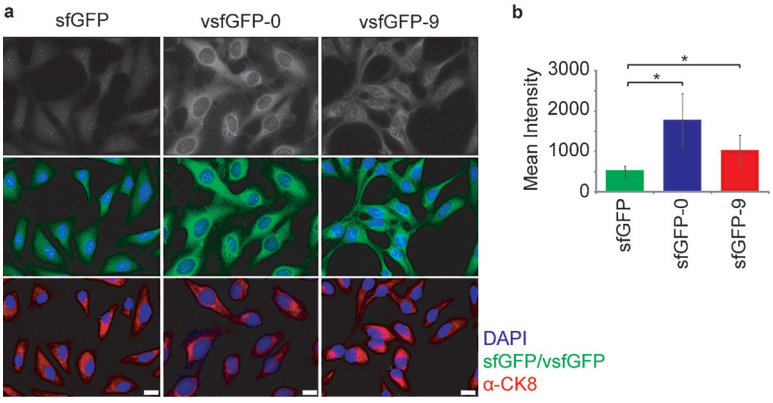

Figure 5. vsfGFP variants outperform sfGFP as fluorophores for an antibody-based molecular probe. a) Fluorescence micrographs (40×) of HeLa cells co-stained with rabbitα-CK8 antibody (red) and an α-CK8 nanobody fused to sfGFP, vsfGFP-0, vsfGFP-9 (green). Nuclei are stained with DAPI (blue). Top row: Grayscale image of the green channel. Middle row: merge of green (nanobody fusions) and blue (nuclei) channels. Bottom row: merge of red (rabbit α-CD8) and blue (nuclei) channels (scale bar, 20 μm). Illumination and capture parameters were constant for all images of the green channel; illumination and capture parameters were optimized for each image of the blue and red channels. b) Mean of raw pixel intensities in the green (nanobody fusions) channel within a 15 pixel region surrounding nuclei. Error bars represent standard deviations. *, $p < 0.00001$ (Student's t-test).

(0 h) to 5.5 (6 h), which we did observe in FACS data in vivo (Figure 6c). We also fused sfGFP and vsfGFP-9 to a peroxisomal localization signal; vsfGFP-9 gave similar localization and higher brightness and stability compared to sfGFP (Figure S10). Thus, vsfGFP-9 performs similarly to sfGFP as a protein fusion partner in vivo with the advantage of improved pH robustness.

In summary, we have invented the "vGFP strategy", incorporating GFP-binding nanobodies and rational structural design. Using vsfGFP, we demonstrated control of dimerization, 7- to 8-fold increased pH resistance, and higher brightness in in vitro and in vivo applications. Furthermore, brightness is concordant across all assays from single molecule to in vivo applications. The structural basis for improved brightness and acid resistance relies on stabilization of otherwise unfavorable protein conformations (i.e. movement of His-148 of sfGFP) by the bound nanobody, suggesting that binding proteins in general may be used to alter other protein properties. Such complexes can then be further improved by directed evolution. We term this strategy "Landscape Expansion", leveraging the stability of nanobody binding for improvements, which is conceptually related to stability-mediated epistasis observed in other directed evolution experiments.[16]

Acknowledgements

This research was supported by the National Research Foundation, Prime Minister's Office, Singapore under its NRF Research Fellowship Scheme (NRF Award No. NRF-RF2010-10) and the Genome Institute of Singapore (GIS)/ Agency for Science, Technology and Research (A*STAR). G.S. was supported by the National University of Singapore; T.W. by the Singapore Ministry of Education (MOE2012-T2-1-101/R-154-000-543-112); A.G. and G.J. by the German Science Foundation (DFG JU650/5-1); and R.J. by the MOST China-EU Science and Technology Cooperation Program, Grant No. 2013DFE33080, the National Natural Science Foundation of China (Grant no. 31471238), and a 100 talent award of the Chinese Academy of Sciences. Howard Robinson helped with crystal data collection and processing at beamline X29 of the National Synchrotron Light Source, supported by the Offices of Biological and Environmental Research and of Basic Energy Sciences of the US Department of Energy, the National Center for Research Resources (P41RR012408), and the National Institute of General Medical Sciences (P41GM103473) of the National Institutes of Health. Said Eshaghi helped with SEC-MALLS analysis, Robert Robinson with protein purification, Lawrence Stanton with cell culture reagents, Jagadish Sankaran with extinction coefficient measurements, and Foo Yong Hwee and the SBIC-Nikon Imaging Centre at Biopolis with photobleaching experiments.

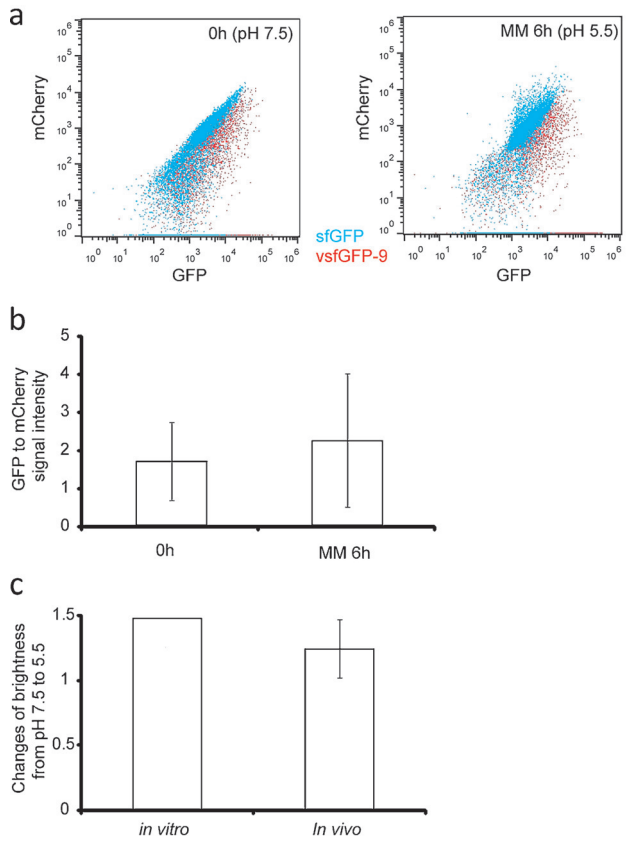

Figure 6. vsfGFP-9 is an effective fusion partner with improved pH robustness in vivo. a) Flow cytometry analysis of transfected 293T cells with mCherry_sfGFP_LC3 (blue) and mCherry_vsfGFP-9_LC3 (red), before (0 h) and after exposure to minimal medium (MM) supplemented with 5 μM PP242 for 6 h. Scatter plots indicate the mCherry (*Y*-axis) and GFP (*X*-axis) fluorescence for individual cells. b) Ratio of median GFP fluorescence (normalized to median mCherry fluorescence) of vsfGFP-9 to sfGFP. For each protein fusion, median GFP signal was divided by median mCherry signal in panel (a) to obtain normalized GFP fluorescence; the ratio of the normalized GFP fluorescence for vsfGFP-9 to sfGFP is plotted here. c) Additional increase in brightness of vsfGFP-9 compared with sfGFP as pH changes from 7.5 to 5.5. Left bar is calculated based on the in vitro FCS data from Figure 3. Right bar is calculated as the ratio of the in vivo values plotted in panel (b). Error bars shows standard deviations between three independent experiments.

Keywords: dimerization · fluorescent probes · green fluorescent protein · protein engineering · single-molecule studies

How to cite: *Angew. Chem. Int. Ed.* **2015**, *54*, 13952–13956
Angew. Chem. **2015**, *127*, 14158–14162

[1] J. Zhang, R. E. Campbell, A. Y. Ting, R. Y. Tsien, *Nat. Rev. Mol. Cell Biol.* **2002**, *3*, 906.
[2] S. p. Cabantous, T. C. Terwilliger, G. S. Waldo, *Nat. Biotechnol.* **2005**, *23*, 102.
[3] J. L. Casey, A. M. Coley, L. M. Tilley, M. Foley, *Protein Eng.* **2000**, *13*, 445.
[4] E. Snapp, *Curr. Protoc. Cell Biol.* **2005**, *21*.4. 1.
[5] R. Y. Tsien, *Annu. Rev. Biochem.* **1998**, *67*, 509.
[6] K. Morino, H. Katsumi, Y. Akahori, Y. Iba, M. Shinohara, Y. Ukai, Y. Kohara, Y. Kurosawa, *J. Immunol. Methods* **2001**, *257*, 175.
[7] P. Chames, M. Van Regenmortel, E. Weiss, D. Baty, *Br. J. Pharmacol.* **2009**, *157*, 220.
[8] U. Rothbauer, K. Zolghadr, S. Muyldermans, A. Schepers, M. C. Cardoso, H. Leonhardt, *Mol. Cell. Proteomics* **2008**, *7*, 282.
[9] K. Schmidthals, J. Helma, K. Zolghadr, U. Rothbauer, H. Leonhardt, *Anal. Bioanal. Chem.* **2010**, *397*, 3203.
[10] J. C. Tang, T. Szikra, Y. Kozorovitskiy, M. Teixiera, B. L. Sabatini, B. Roska, C. L. Cepko, *Cell* **2013**, *154*, 928.
[11] A. Kirchhofer, J. Helma, K. Schmidthals, C. Frauer, S. Cui, A. Karcher, M. Pellis, S. Muyldermans, C. S. Casas-Delucchi, M. C. Cardoso, *Nat. Struct. Mol. Biol.* **2010**, *17*, 133.
[12] R. A. Griep, C. van Twisk, J. M. van der Wolf, A. Schots, *J. Immunol. Methods* **1999**, *230*, 121.
[13] A. L. Olichon, T. Surrey, *J. Biol. Chem.* **2007**, *282*, 36314.
[14] U. Rothbauer, K. Zolghadr, S. Tillib, D. Nowak, L. Schermelleh, A. Gahl, N. Backmann, K. Conrath, S. Muyldermans, M. C. Cardoso, *Nat. Methods* **2006**, *3*, 887.
[15] C. Branden, J. Tooze, *Introduction to protein structure*, *Vol. 2*, Garland, New York, **1991**.
[16] J.-D. Pédelacq, S. Cabantous, T. Tran, T. C. Terwilliger, G. S. Waldo, *Nat. Biotechnol.* **2006**, *24*, 79.
[17] U. Haupts, S. Maiti, P. Schwille, W. W. Webb, *Proc. Natl. Acad. Sci. USA* **1998**, *95*, 13573.
[18] J. Widengren, Ã. Mets, R. Rigler, *Chem. Phys.* **1999**, *250*, 171.
[19] "Brighter fluorescent derivatives of UTI89 utilizing a monomeric vGFP": M. Eshaghi, K. Mehershahi, S. Chen, *Pathogen*, **2015**, accepted.
[20] U. Rothbauer, K. Zolghadr, S. Tillib, D. Nowak, L. Schermelleh, A. Gahl, N. Backmann, K. Conrath, S. Muyldermans, M. C. Cardoso, H. Leonhardt, *Nat. Methods* **2006**, *3*, 887.
[21] Y. Kabeya, N. Mizushima, T. Ueno, A. Yamamoto, T. Kirisako, T. Noda, E. Kominami, Y. Ohsumi, T. Yoshimori, *EMBO J.* **2000**, *19*, 5720.
[22] S. Kimura, T. Noda, T. Yoshimori, *Autophagy* **2007**, *3*, 452.
[23] N. Demaurex, *Physiology* **2002**, *17*, 1.
[24] W. W. Ward, S. H. Bokman, *Biochemistry* **1982**, *21*, 4535.
[25] G. H. Patterson, S. M. Knobel, W. D. Sharif, S. R. Kain, D. W. Piston, *Biophys. J.* **1997**, *73*, 2782.

Received: July 20, 2015
Revised: September 10, 2015
Published online: October 8, 2015